Nonlinear Haptic Rendering of Deformation and Cutting Based on Orthogonal Decomposition

Gabriel Sepúlveda¹, Vicente Parra², Omar Domínguez³

- Departamento de Ingeniería Eléctrica, CINVESTAV, México DF gsepulveda@cinvestav.mx
- ² Grupo de Robótica y Manufactura Avanzada, CINVESTAV, Saltillo vparra@cinvestav.mx
- Gentro de Investigación en Tecnologías de Información y Sistemas, UAEH, Pachuca, México omar_arturo@uaeh.edu.mx

(Paper received on February 29, 2008, accepted on April 15, 2008)

Abstract. This document presents a new method for the induction of nonlinear dynamics for deforming and cutting virtual objects using haptic devices. The properties of the virtual objects are obtained of bio-mechanical characterization reported in the literature. The dynamics are generated over differentiable manifolds defined by implicit functions and using the orthogonal decomposition of the haptic device dynamic. An exponential bio-mechanic model of liver tissue during deformation is implemented along with an energetic model of cutting based on fracture mechanical approach. The experimental results are presented within a platform running with a 3DOF haptic device and a 3D environment showing a stable interaction.

1 Introduction

Modeling the dynamic properties of different kind of tissues during deformation and cutting is an essential task for developing a surgery simulator that pretends to approximate the perception of the user to the reality. The more realistic the model programmed is, the more accurate the force feedback is computed during the simulation using a haptic device. The bio-mechanical properties of tissues during deformation and cutting are generally nonlinear mathematic models. A haptic engine that allows the recreation of this kind of dynamic models is needed to accomplish the task.

An approach using mass-spring-damper(MSD) model system are shown in [1]. An approach based on the bookkeeping of force deflections curves stored at the nodes of a triangulated body surface is presented in [2] and [3]. An energetic model of interaction during cutting of samples of potato and real pig's liver tissue is presented in [4]. A nonlinear dynamic model due to friction, deformation and cut during needle insertion is presented in \cite{aguja2}. A cutting model approach using Local Element Method (LEM) is presented in [5]. An exponential model of deformation, of in-vivo and ex-vivo pig tissues, is obtained in \cite{In-vivo} using specific devices to measure tissue properties under extension and indentation, as well as to record instrument-tissue interaction forces. To produce realistic behavior in virtual environment simula-

© E. V. Cuevas, M. A. Perez, D. Zaldivar, H. Sossa, R. Rojas (Eds.) Special Issue in Electronics and Biomedical Informatics, Computer Science and Informatics
Research in Computing Science 35, 2008, pp. 51-61



tions for surgical training, it is important to have a haptic engine that allows the recreation of this models and characterization using a haptic device.

1.1 Contributions

Arimoto [8] presented a method for orthogonal decomposition of the forces during the interaction between a robot manipulator and an infinitely rigid object. We propose a new methodology based on this orthogonal decomposition applied over a haptic device's dynamics, enabling the implementation of a control law that generates different kinds of dynamic models for haptic rendering virtual object's dynamics, this new method permits the simultaneous generation of contact forces like deformation and cutting and surfaces properties like tangent friction. In this paper a nonlinear deformation model and tissue cutting characterization model are presented along with simple surface properties for virtual objects. The models presented in [7] and [4] are implemented using Phantom Premium haptic device [9]. The human-in-the-loop experimental interaction results are presented with a discussions an future work.

2 Dynamic induction using orthogonal decomposition

A methodology that allows the orthogonal decomposition of the dynamic of a haptic device is presented in [10], and the most important issues are dicussed here.

The dynamic of a haptic device is modeled as chained linked robot:

$$H(q)\ddot{q} + C(q, \dot{q})\dot{q} + q(q) = \tau + \tau_h \tag{1}$$

$$\tau_h = J^T F \tag{2}$$

where $q,q\in\Re^n$ are vectors that represents the articular position and velocities, n is the number of degrees of freedom (DOF), $H(q)\in\Re^{n\times n}$ is a matrix representing the inertial forces of the haptic device with $H(q)=H(q)^T$ positive defined, $H(q)\in\Re^{n\times n}$ is the Coriolis forces matrix with H(q)-2C(q,q) an antisymmetric matrix, $g(q)\in\Re^n$ is the gravitational force vector, $\tau\in\Re^n$ is the input torques vector, $J\in\Re^n$ is the haptic device's analytic Jacobian, $F_h\in\Re^3$ is the human input force, $\tau_h\in\Re^n$ represents the input torques due to F_h .

The virtual object's dynamic properties are generated by two manifolds defined as an implicit functions of the articular variables q as follows:

$$V_0 = \{ q \in \mathfrak{R}^n \mid \varphi(q) = 0 \}$$
 (3)

$$V_{psi} = \{ q \in \Re^n \mid \psi(q) = 0 \}$$
 (4)

with $\varphi(q):V_o\to\Re$ called object manifold and $\psi(q):V_o\to\Re^n$ called psi manifold.

The orthogonal decomposition of the haptic device's dynamic is achieved applying the following control law:

$$\tau_1 = C(q, q)q + g(q) - PH(q)J_{\varphi^*}J_{\varphi}q - QH(q)Qq - J_{\varphi}^T \lambda_d - Q\zeta_d$$
 (5)

$$P = \frac{J_{\varphi}^{T} J_{\varphi}}{J_{\varphi} J_{\varphi}^{T}} \tag{6}$$

where J_{φ} and Q are the jacobian matrices of functions $\varphi(q)$ and $\psi(q)$ respectively, J_{φ^*} is the pseudo inverse of J_{φ} . The variables λ_d and ζ_d are used to induce the dynamics and surface properties of the virtual object as is presented later in this document.

Substituting (5) in (1) and using the analysis presented in [10] the close loop equation that is to be analyzed is:

$$\varphi(q) = M_{\varphi}(\lambda - \lambda_d) \tag{7}$$

$$\psi(q) = M_{\psi}(\zeta - \zeta_d) \tag{8}$$

with

$$M_{\sigma} = J_{\sigma} H(q)^{-1} J_{\sigma}^{T} \tag{9}$$

$$M_{\scriptscriptstyle W} = QH(q)^{-1}Q \tag{10}$$

3 Exponential deformation model

For recreating the correct force feedback during interaction with nonlinear dynamic object like organic tissue, it is important to implement mathematic models that represents the properties of the real tissue. One form to accomplish this task is to implement the bio-mechanical models obtained form direct experiments.

A mathematical model of pig's abdominal tissues is presented in [7], the biomechanical characterization is done using surgery tools coupled with sensors during deformation. The mathematic model is:

$$F = \alpha e^{\beta \sigma} \tag{11}$$

where F is the reaction force, α and β are specific constants for each kind of tissue, σ represents the stretch ratio during deformation. For pig intestine sample the values reported in [7] are $\alpha=3.7\times10^{-9}$ and $\beta=9.4$ for ex-vivo experiments and $\alpha=4.3\times10^{-7}$ and $\beta=13$ for in-vivo experiments. To induce this behavior the variable λ_d is defined as follows:

$$\lambda_{d1} = -M_{\varphi}^{-1} B_0 \phi(q) + M_{\varphi}^{-1} \alpha e^{-\beta \frac{\phi(q)}{L_0}}$$
(12)

where α, β are the constants reported in [7] and L_0 represents the sample's thickness in the direction of the compression force, B_0 is a defined positive constant that represents the virtual object's viscosity coefficient, used to induce stability to the whole system. The sign within the exponential is because the value of $\varphi(q)$ is negative inside the virtual object. Substituting (12) in (7) we obtain the following dynamic system:

$$\varphi(q) + B_0 \varphi - \alpha e^{-\beta \frac{\varphi(q)}{L_0}} = M_{\varphi} \lambda$$
 (13)

The implementation of tangent friction is achieved through the variable ζ_d as follows:

$$\zeta_d = B_1 \psi(q) \tag{14}$$

where B_1 is a diagonal matrix with all positive values b_1 . Substituting (14) in (8) the following system is obtained:

$$\psi(q) = M_{\psi} \zeta - M_{\psi} B_1 \psi(q) \tag{15}$$

4 Cutting model using a fracture mechanics approach

One of the principal task during the interaction with tissue is cutting. An approach of this task is presented in [4] based on fracture mechanical approach, this model presents an energetic interchange between three states: deformation, fracture and cutting.

The analysis in [4] is done considering a rectangular sharp tool as is shown in Fig. 1. The energetic interchange is represented by the following equation:

$$\Delta W_e = \Delta U + \Delta W_s \tag{16}$$

where ΔW_e represents the extern energy applied, ¢U is the change in the elastic potential energy and ΔU is the irreversible work of fracture. During deformation the external energy applied is stored as elastic potential energy, one example of this behavior is the deformation of a linear spring ($E = \frac{1}{2}kx^2$) where the energy applied to the spring is stored and recover when the spring is released, this behavior is presented in the following equation:

$$\Delta W_e = \Delta U \tag{17}$$

If the interaction during deformation reaches a stored energy limit the behavior changes from deformation to fracture interaction, this limit is called the material's yield point. During fracture the elastic potential energy stored instantaneously creates a crack in the object:

$$\Delta W_s = \Delta U \tag{18}$$

During cutting interaction the energy applied increases the depth of the crack done during fracture interaction.

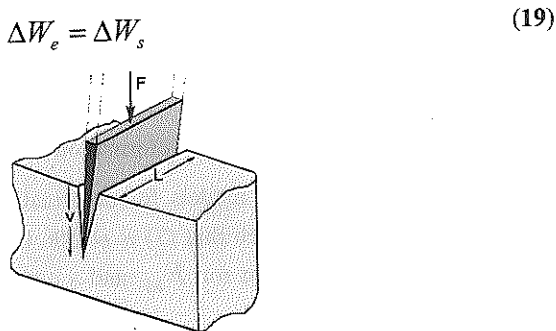


Fig. 1. Tool-body interaction model presented in [4], F represents the force applied, ν represents the penetration depth, and L represents the length of the tool.

The transition between the interaction modes is as follows:

- 1. Without contact the state is considered as free movement.
- Once the virtual tool is in contact with the virtual object the deformation state is present.
- The external force applied stores elastic energy accordingly with the elastic deformation model used.
- The deformation interaction continues until the yield point is reached at this
 point the interaction changes to fracture.

5. The elastic potential energy stored at this point is released creating the crack. If the tool keeps going inside the object the cutting interaction is reached otherwise the state returns to free movement with the new contact surface at the end of the crack.

The procedure is shown in the Fig. 2, where v represents the penetration speed.

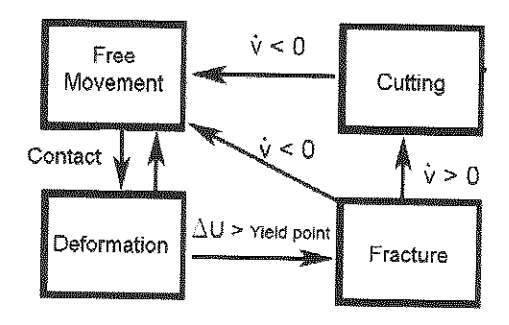


Fig. 2. Interaction modes sequence presented in [4].

To induce this behavior the variable λ_d from (5) is dened for the deformation and cutting interaction modes as follows:

$$\lambda_{d2} = F_{def}(\varphi, \dot{\varphi}) \tag{20}$$

$$\lambda_{d3} = F_c(\varphi, \phi) \tag{21}$$

where λ_{d2} and λ_{d3} are used for deformation and cutting respectively, F_{def} and F_c represents the interaction models for deformation and cutting interactions, this models have to be chosen such that (7) is stable. One example could be the spring-damper model for deformation for F_{def} and a constant force F_c as is presented in [4].

5 Experimental platform

The models presented in this paper are implemented in a computer to simulate nonlinear deformation and cutting interaction. The PC is running at 2.4GHz with AMD Athlon processor, 1Gb RAM, 64Mb NVIDIA Ge Force 4 MX and RedHat Linux 9.0 with real time patch. The user application was developed using Qt [11] for graphical tools and OpenGL and GLU for 3D graphics, the programming language was C++.

Fig. 3. Experimental platform. Left: PC, monitor and haptic device. Right: GUI using a wired virtual hand used as proxy during the interaction with a virtual sphere, the buttons, sliders and text boxes for changing the experimental parameters in-line.

The haptic device used is Phantom Premium [12], the dynamic model is obtained in [13]. The Fig. 3 shows the GUI during the interaction with a virtual sphere along with the tools used to change in line the parameters during the simulation. The graphics of the most important process variables are shown, also a wired hand used as proxy is presented.

6 Experimental results

The experimental results of two interaction models are presented, the first using the exponential deformation and the second using the cutting model both with tangent friction and using a plane as the virtual object. The virtual plane is defined as de XZ plane at the coordinates origin as it is shown in Fig. 4.

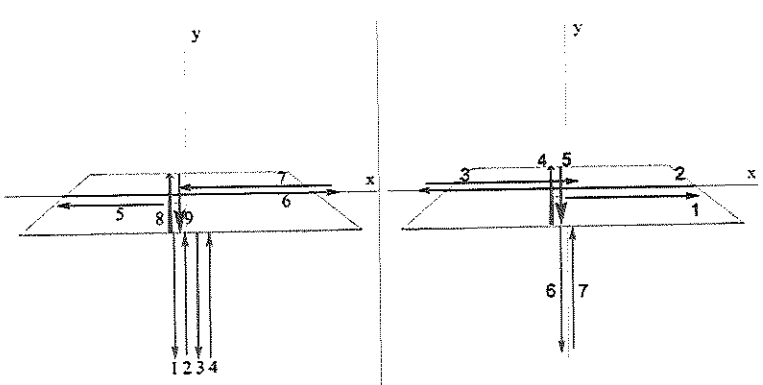


Fig. 4. Displacements during interaction with a virtual plane. Left: displacements order during experiment 1. Right: displacements order during experiment 2. The z axis is considered in direction outside the sheet.

Experiment 1: the experiment starts with the proxy at the origin of cartesian coordinates (x = 0; y = 0; z = 0), the displacements are done using straight lines in the following directions: -y, y, -y, y, -x, x, -x, -z, z. This is shown in Fig. 4 left, where the numbers 1-9 represents the order of the displacements.

Experiment 2: the experiment starts also at the origin of cartesian coordinates, the displacements are done using also straight lines in the following directions: x, -x, x, -z, z, -y until reaching the cutting mode then and finally y. This is shown in Fig. 4 right.

The implementation of the exponential deformation model the equation used was (12) and for the cutting model the following variables were defined:

$$\lambda_{d2} = -M_{\varphi}B_0\phi + M_{\varphi}^T\alpha e^{-\beta\frac{\varphi}{L_0}}$$
 (22)

$$\lambda_{d3} = -2.0 \tag{23}$$

Both experiments use the following parameters: $B_0=20$, $\alpha=4.3\times 10^{-7}$, $\beta=13$, $L_0=0.1$ the tangent friction is induced using (14) con $b_1=0.06$ for experiment 1 and $b_1=0$ for experiment 2.

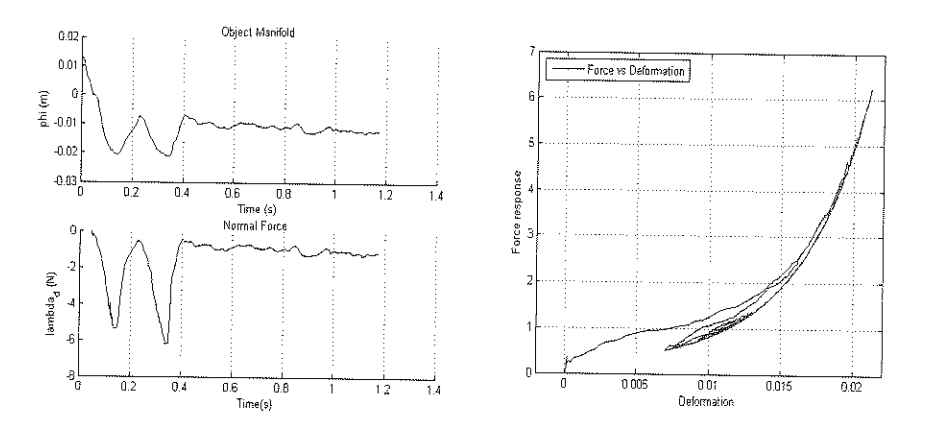


Fig. 5. Experiment 1, interaction with a virtual plane using the exponential deformation model with tangent friction. Left: Object manifold and normal force vs *t*. Right: Deformation vs Force response

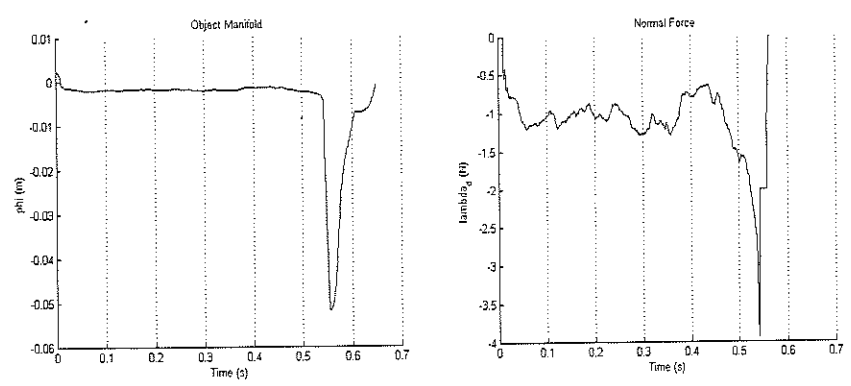


Fig. 6. Experiment 2, interaction with a virtual plane using the exponential deformation and cutting model without tangent friction. Left: Object manifold vs t. Right Normal force vs t.

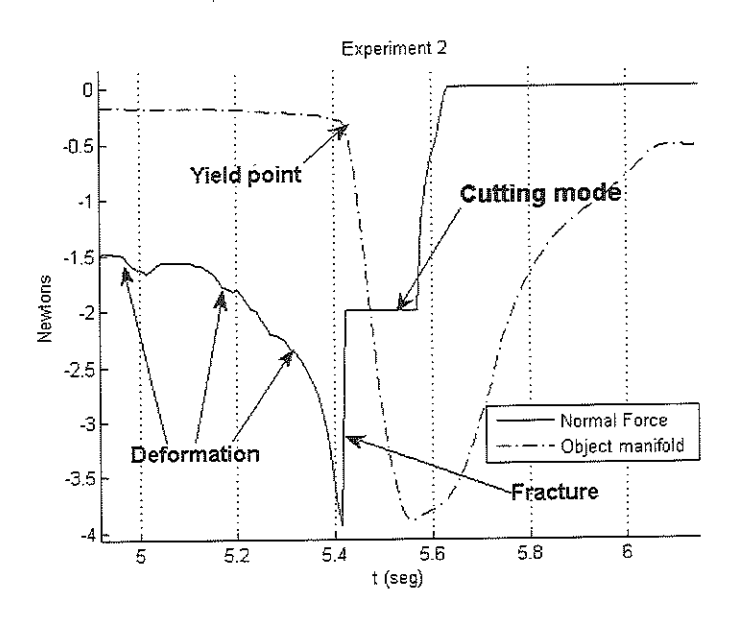


Fig. 7. Transition between the different modes in the cutting algorithm, the reaction force is presented with a filled line and the object manifold with dotted line. The deformation mode is presented until t=5.4128 seconds, then the yield point is reached and the interaction switches to rupture mode for 1 millisecond this is due to the platform's sampling period, then the interaction switches to cutting for 156 milliseconds, in this mode a constant force of -2 Newton is presented, at last the tool moves outside the virtual object and the reaction force is zero.

7 Conclusions

A new methodology for the implementation of bio-mechanical characterization for the interaction with a virtual object simultaneously with surface properties, using a haptic device has been tested presenting a high performance on a low end computer. The experimental results using two different interaction models, exponential deformation Fig. 5 and cutting interaction Fig. 6, presented in the literature is shown. An extended explanation of the interaction during cutting is explained in Fig. 7, where it could be seen the four interaction models presented in [4]: Free motion, deformation, fracture creation and cutting.

The methodology could be implemented to any nonlinear bio-mechanical model as long as it could be expressed in terms of the depth penetration and penetration speed. Complex surfaces properties could also be implemented. The extension to any arbitrary object form could be implemented as long as it could be expressed with a set of implicit equations. The experiments were done during a human-in-the-loop interaction showing a stable behavior in a low end experimental platform.

8 Future work

The future work will be to implement complex surface properties like textures and advanced friction models for making more realistic the interaction. Also the implementation of complex objects defined by a set of implicit equations is the next step. The implementation of the methodology using different haptic devices is at hand.

9 Acknowledgment

The authors thank to CONACYT, CINVESTAV Cd. de México, CINVESTAV Saltillo and CITIS UAEH, Hidalgo México.

References

- Cagatay Basdogan et al. Simulation of tissue cutting and bleeding for laparascopic surgery using auxiliary surfaces. Technical report, Cambridge, MIT, USA.
- Nicholas Ayache Stéphane Cotin, Hervé Delingette. A hybrid elastic model allowing real-time cutting, deformation and force feedback for surgery training and simulation. INRIA, 2004.
- Mohsen Mahvash & Vincent Hayward. High-fidelity passive force-reflecting virtual environments. IEEE Transactions on Robotics, pages 38-46, 2005.
- Mohsen Mahvash & Vincent Hayward. Haptic rendering of cutting: A fracture mechanics aproach. Technical report, McGill University, Quebec, Canada, 2001.

- 5. Allison M. Okamura. Force modeling for needle insertion into soft tissue. IEEE TRANSACTIONS ON BIOMEDICAL ENGINEERING, 51(10), October 2004.
- 6. Teeranoot Chanthasopeephan Jaydev P. Desai and Alan C. W. Lau. 3d and 2d finite element analysis in soft tissue cutting for haptic display. ICAR, pages 360-
- 7. Iman Brouwer et al. Measuring in vivo animal soft tissue properties for haptic modeling in surgical simulation. Technical report, University of California, USA,
- 8. Suguru Arimoto. Control Theory of Non-linear Mechanical Systems. Oxford Science Publications, 1 edition, 1996.
- SensAble Technologies Inc. Phantom premium 1.0/1.5a, 3d touch components: Hardware installation and technical manual, ver 6.5, August 2000.
- 10. Gabriel Sepúlveda Vicente Parra and Omar Domínguez. A high performance haptic rendering method based on orhogonal decomposition of haptic device's dynamics. Subminited to IEEE Transaction on Haptics, 2008.
- 11. http://trolltech.com/products/qt.
- 12. SensAble Technologies Inc. Specifications for the phantom ® omni haptic device, March 2004.
- 13. Omar Arturo Domínguez Ramírez. Design and integration of a Realistic Haptic Interface. Phd thesis, CINVESTAV, Mechatronic Section, México,